Thermal convection in inclined cylindrical containers

Shishkina, O. & Horn, S.

Author post-print (accepted) deposited by Coventry University's Repository

Original citation & hyperlink:
Shishkina, O & Horn, S 2016, 'Thermal convection in inclined cylindrical containers' Journal of Fluid Mechanics, vol. 790.
https://dx.doi.org/10.1017/jfm.2016.55

DOI 10.1017/jfm.2016.55
ISSN 0022-1120
ESSN 1469-7645

Publisher: Cambridge University Press

Copyright © and Moral Rights are retained by the author(s) and/ or other copyright owners. A copy can be downloaded for personal non-commercial research or study, without prior permission or charge. This item cannot be reproduced or quoted extensively from without first obtaining permission in writing from the copyright holder(s). The content must not be changed in any way or sold commercially in any format or medium without the formal permission of the copyright holders.

This document is the author's post-print version, incorporating any revisions agreed during the peer-review process. Some differences between the published version and this version may remain and you are advised to consult the published version if you wish to cite from it.

Thermal convection in inclined cylindrical containers

Olga Shishkina[1]† and Susanne Horn[2]

[1]Max Planck Institute for Dynamics and Self- Organization, Am Fassberg 17, D-37077 Göttingen, Germany

[2]Department of Mathematics, Imperial College London, London SW7 2AZ, UK

(Received xx; revised xx; accepted xx)

By means of Direct Numerical Simulations (DNS) we investigate the effect of a tilt angle β, $0 \leqslant \beta \leqslant \pi/2$, of a Rayleigh–Bénard convection (RBC) cell of the aspect ratio 1, on the Nusselt number Nu and Reynolds number Re. The considered Rayleigh numbers Ra are from 10^6 to 10^8 and Prandtl numbers are from 0.1 to 100 and the total number of the studied cases is 108. We show that the $Nu(\beta)/Nu(0)$ dependence is not universal and is strongly influenced by a combination of Ra and Pr. Thus, with a small inclination β of the RBC cell, the Nusselt number can decrease or increase, compared to that in the RBC case, for large and small Pr, respectively. A slight cell tilting may not only stabilise the plane of the large-scale circulation (LSC) but can also enforce one for cases when the preferred state in the perfect RBC case is not an LSC but a more complicated multiple roll state. Close to $\beta = \pi/2$, Nu and Re decrease with growing β in all considered cases. Generally, the $Nu(\beta)/Nu(0)$ dependence is a complicated, non-monotonic function of β.

Key words: Bénard convection, Convection in cavities, Turbulent convection

1. Introduction

Fluid motion driven by an imposed temperature gradient is a common phenomenon in nature and is important in many industrial applications. In the classical models of thermal convection, i.e. Rayleigh–Bénard convection (RBC) and vertical convection (VC), the fluid is confined between a heated and a cooled plate which are parallel to each other. The induced flow is determined by the Rayleigh number $Ra \equiv \alpha g \Delta H^3/(\kappa\nu)$, Prandtl number $Pr \equiv \nu/\kappa$ and the aspect ratio of the container $\Gamma \equiv D/H$. Here α denotes the isobaric thermal expansion coefficient, ν the kinematic viscosity, κ the thermal diffusivity of the fluid, g the acceleration due to gravity, $\Delta \equiv T_+ - T_-$ the temperature difference between the warm (T_+) and the cold (T_-) isothermal boundaries. We will only consider cylindrical vessels, characterised by the diameter D and the distance H between the heated and cooled plates.

The essential difference between RBC and VC is the direction of the gravity vector, i.e. it is parallel to the isothermal surfaces of the container in the case of VC and perpendicular to them in RBC. However, the respective flows are different and the Reynolds number Re and the mean heat flux, described by the Nusselt number Nu, exhibit very different dependencies on Ra and Pr. For reviews on these two classical convection models, we refer to Ahlers *et al.* (2009); Bodenschatz *et al.* (2000); Castaing

† Email address for correspondence: Olga.Shishkina@ds.mpg.de

et al. (1989); Chillà & Schumacher (2012); Lohse & Xia (2010); Siggia (1994) and to Ng *et al.* (2015), respectively.

Experimental studies of turbulent thermal convection in long cylinders filled with low-Prandtl-number fluids show that the convective heat transfer between the heated and cooled parallel surfaces of the container is most effective neither in a standing position of the cylinder (as in RBC, with a cell inclination angle $\beta = 0$), nor in a lying position (as in VC, $\beta = 0.5\pi$), but in an inclined container, for a certain intermediate value of β, $0 < \beta < 0.5\pi$. Such measurements in liquid sodium, $Pr \sim 0.01$, are reported by Frick *et al.* (2015); Kolesnichenko *et al.* (2015); Vasil'ev *et al.* (2015). Moreover, these experiments show that in the case of small Pr ($Pr \ll 1$) and relatively large Ra ($Ra \gtrsim 10^9$), any tilt β, $0 < \beta \leqslant \pi/2$, of the cell leads to an increase of Nu, compared to that in the RBC case ($\beta = 0$). Langebach & Haberstroh (2014) also obtained similar results in their experimental study for $Pr \approx 0.7$.

The effect of the cell tilting on convective heat transport in large-Prandtl-number fluids is very different from that in the case of low-Prandtl-number fluids. Thus, experiments by Guo *et al.* (2015) in a parallelepiped container for $Pr \approx 6.7$ and $Ra \approx 4.4\times10^9$ showed a monotonic reduction of Nu with increasing β in $\beta \in [0, \pi/2]$.

One should note that most of the investigations of the cell-tilt effects on the mean heat transport were conducted in a narrow region of β close to 0 and mainly for $Pr > 1$. These studies show generally a small effect of the cell inclination on the mean heat transport (Ciliberto *et al.* 1996; Cioni *et al.* 1997; Roche *et al.* 2010; Ahlers *et al.* 2006; Wei & Xia 2013). Measurements by Chillà *et al.* (2004) for $0 < \beta \lesssim 0.01\pi$ and $5 \times 10^{11} \leqslant Ra \leqslant 4 \times 10^{12}$ in a cylindrical container of $\Gamma = 1/2$, filled with hot water, $Pr \approx 2$, showed a reduction of the normalized Nusselt number $Nu(\beta)/Nu(0)$ approximately as $1 - 2\beta$, if a two-roll global flow structure developed. For $Pr \approx 4.3$ and $3 \times 10^9 \lesssim Ra \lesssim 7 \times 10^{10}$ Sun *et al.* (2005) also found a reduction of Nu if their cylindrical ($\Gamma = 1/2$) RBC cell was tilted for $\beta \approx 0.01\pi$. As the Nu-reduction with the cell tilt was associated with the development of a two-roll flow structure, no significant Nu-reduction was expected in a slightly inclined cell of $\Gamma = 1$. Measurements by Ahlers *et al.* (2006) in a $\Gamma = 1$ cylindrical cell filled with water ($Pr \approx 4.3$) for Rayleigh numbers about 10^{11} showed indeed only a tiny reduction of Nu, namely as $Nu(\beta)/Nu(0) \approx 1 - 0.03\beta$, and a much stronger Reynolds-number dependence $Re(\beta)/Re(0) \approx 1 + 1.85\beta - 5.9\beta^2$. For similar Pr, $\Gamma = 1/2$ and $Ra = 1.8 \times 10^{10}$ and 7.2×10^{10}, Weiss & Ahlers (2013) found even a very small increase of the mean heat transport with the local maximum at $\beta \approx 0.02\pi$. This increase was explained by a stabilization of the single-roll state of the large-scale circulation (LSC) and a destabilization of the double-roll state, which are associated with, respectively, an increase and decrease of the mean heat transport. From all these experimental results one can already conclude that the $Nu(\beta)/Nu(0)$ dependence near $\beta = 0$ is strongly dependent on Ra, Pr and Γ and is a complicated function of these parameters, which cannot be represented as a simple product of their power functions.

In the present study, we investigate the effect of a cell tilt, reflected in the inclination angle β, $0 \leqslant \beta \leqslant \pi/2$, on the Nusselt and Reynolds numbers by means of Direct Numerical Simulations (DNS) of thermal convection in a cylindrical vessel with aspect ratio 1.

2. Results

The following combinations of Ra and Pr were considered in our three-dimensional DNS: $Ra = 10^6$ for $Pr = 0.1$, 1, 10 and 100; $Ra = 10^7$ for $Pr = 1$ and 10; and $Ra = 10^8$ for $Pr = 1$. For each combination of Ra and Pr we studied thermal convection under the

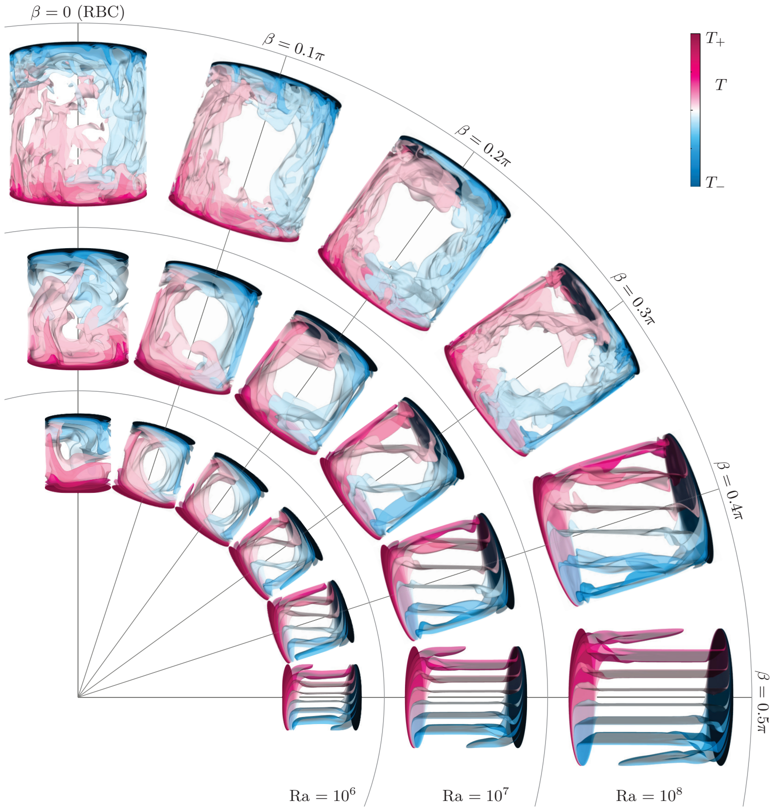

FIGURE 1. Isosurfaces of the instantaneous temperature fields in inclined convection in cylindrical containers filled with a fluid of $Pr = 1$, for $Ra = 10^6$, 10^7, 10^8 and different inclination angles $\beta = 0$, 0.1π, 0.2π, 0.3π, 0.4π and 0.5π, as obtained in our DNS. Shown are ten isosurfaces that are equidistantly distributed between the heated (T_+) and cooled (T_-) cell boundaries. The proportions between the different sizes of the presented convection cells reflect the proportions between the different Ra.

Oberbeck–Boussinesq approximation, in inclined cylindrical containers with $\Gamma = 1$ and with different inclination angles β that varied between 0 (RBC) and $\pi/2$ (VC). Thus, the problem is governed by the Navier–Stokes equations in cylindrical coordinates (r, ϕ, z):

$$\begin{aligned} \boldsymbol{\nabla} \cdot \boldsymbol{u} &= 0, \\ D_t \boldsymbol{u} &= \nu \boldsymbol{\nabla}^2 \boldsymbol{u} - \boldsymbol{\nabla} p + \alpha g (T - T_0) \hat{\boldsymbol{e}}, \\ D_t T &= \kappa \boldsymbol{\nabla}^2 T, \end{aligned}$$

where D_t denotes the substantial derivative, $\boldsymbol{u} = (u_r, u_\phi, u_z)$ the velocity vector, p the reduced kinetic pressure, T the temperature, $T_0 = (T_+ + T_-)/2$ and $\hat{\boldsymbol{e}}$ is the unit vector, $\hat{\boldsymbol{e}} = (-\sin(\beta)\cos(\phi), \sin(\beta)\sin(\phi), \cos(\beta))$. These equations are non-dimensionalized by using the cylinder radius R and the quantities $(\alpha g R \Delta)^{1/2}$, $R(\alpha g R \Delta)^{-1/2}$ and Δ as units of length, velocity, time and temperature, respectively. (Note that in the definition of Ra, not the cylinder radius R, but the cylinder height H is used as reference length.)

The resulting dimensionless equations are solved numerically with the code GOLDFISH, as in Shishkina & Wagner (2016); Shishkina *et al.* (2015). The computational grids of up to $(N_r, N_\phi, N_z) = (192, 512, 384)$ nodes satisfy the resolution requirements for DNS (Shishkina *et al.* 2010).

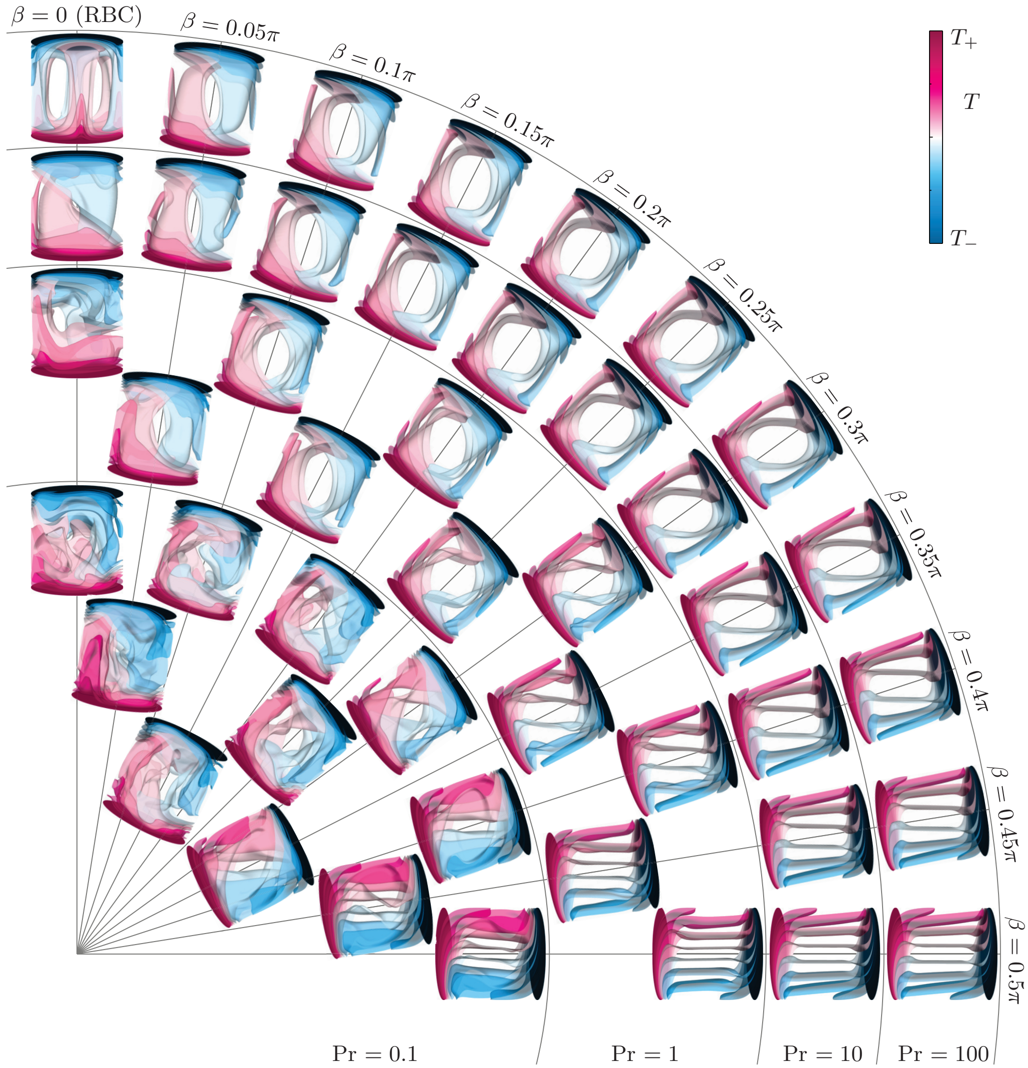

FIGURE 2. Isosurfaces of the instantaneous temperature fields in inclined convection in cylindrical containers, filled with a fluid of $Pr = 0.1$, $Pr = 1$, $Pr = 10$ or $Pr = 100$, for $Ra = 10^6$ and different inclination angles from $\beta = 0$ to $\beta = 0.5\pi$, as obtained in our DNS. Shown are ten isosurfaces that are equidistantly distributed between the heated (T_+) and cooled (T_-) cell boundaries.

The stepping in the β-range varies from 0.0025π to 0.05π, with minimum 11 and maximum 22 different inclination angles between 0 (RBC) and $\pi/2$ (VC). The refined β-resolution is applied for cases that are near $\beta = 0$. This helps to better understand the behaviour of Nu and Re in inclined convection close to the exact RBC case, which is particularly relevant for experimental set-ups. In total we studied 108 different combinations of Ra, Pr and β.

In figure 1 isosurfaces of the instantaneous temperature are presented for $Pr = 1$ and $Ra = 10^6$, 10^7 and 10^8, and 6 particular inclination angles $\beta = 0$ (RBC), 0.1π, 0.2π, 0.3π, 0.4π and 0.5π (VC). In the RBC set-up ($\beta = 0$) the flows are always unsteady or even turbulent, and due to the aspect ratio of $\Gamma = 1$ and relatively small Pr, the global flow

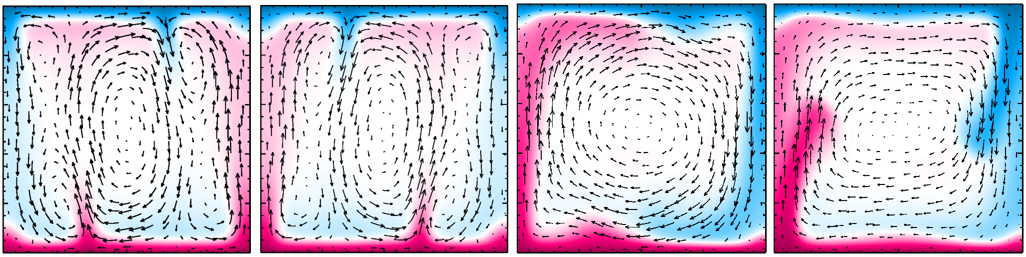

$\beta = 0$ $\beta = 0.0025\pi$ $\beta = 0.0050\pi$ $\beta = 0.0075\pi$

FIGURE 3. Changing of the instantaneous temperature fields with a small inclination angle β for $Pr = 100$ and $Ra = 10^6$. Colour scale as in figure 2.

structure is a large-scale circulation (LSC) filling the whole cell. However, the orientation of the LSC is not fixed and changes with time (e.g. Brown & Ahlers 2006).

With a small inclination β the LSC is fixed to the inclination plane and likewise is its rotation direction. The flow is reorganised in such a way that fluid near the heated (cooled) plate ascends (descends) closer to the sidewall, hence most of the interior fluid is almost quiescent and has a mean temperature of about $T = (T_+ + T_-)/2$. For $\beta \gtrsim 0.3\pi$ the interior temperature field shows signs of stratification, i.e. the temperature isosurfaces align horizontally. Further, with growing β the corner rolls are less pronounced (if exist) and the flow generally stabilizes. Thus, we observe steady flows for $Ra = 10^6$ if $\beta \gtrsim 0.2\pi$, for $Ra = 10^7$ if $\beta \gtrsim 0.3\pi$ and even for $Ra = 10^8$ if $\beta \gtrsim 0.45\pi$. However, with increasing Ra and $\beta = 0.5\pi$ (VC) the up-flow and down-flow along the isothermal plates becomes more vigorous and the impinging of the flow on the viscous boundary layer adjacent to the adiabatic wall leads to distinct overshoots in the temperature and will ultimately lead to a rolling up of the fluid and instability.

Furthermore, we conducted DNS for $Pr = 0.1$, 1, 10 and 100 for a fixed $Ra = 10^6$ (see figure 2) to investigate, how the cell tilt influences convection in fluids with different Pr. For $\beta = 0$ the LSC develops in a singe large-roll state if Pr is small, while for large Pr ($Pr = 100$) a more complicated global flow structure develops (Horn *et al.* 2013; Horn & Shishkina 2014). With a tiny inclination angle β the flow is reorganized in a one-roll LSC even if Pr is large. Thus, for $Pr = 100$, we observe this already for $\beta = 0.005\pi (= 0.9^\circ)$, see figure 3. Again, all flows are stabilized with growing β. For $Ra = 10^6$, $\Gamma = 1$, $\beta = 0$ and all considered Pr the flows are unsteady, but already for $\beta \gtrsim 0.06\pi$ ($Pr = 100$), $\beta \gtrsim 0.15\pi$ ($Pr = 10$), $\beta \gtrsim 0.2\pi$ ($Pr = 1$) and $\beta \gtrsim 0.4\pi$ ($Pr = 0.1$) steady convective flows are observed.

Quantitative characteristics of the inclined convection flows, i.e. the Nusselt number,

$$Nu(z) \equiv (\langle u_z T \rangle_z - \kappa \partial_z \langle T \rangle_z)/(\kappa \varDelta / H) = \text{const.}, \tag{2.1}$$

and the Reynolds number,

$$Re \equiv \sqrt{\langle \mathbf{u} \cdot \mathbf{u} \rangle} H/\nu \tag{2.2}$$

for different Pr are presented in figure 4. Here, $\langle \cdot \rangle_z$ denotes the temporal and planar average at distance z from the heated plate and $\langle \cdot \rangle$ denotes the average in time and over the whole convection cell.

The curves $Nu(\beta)$ for small Pr ($Pr = 1$ and $Pr = 0.1$) and large Pr ($Pr = 10$ and $Pr = 100$) look very different (see figure 4a). In the small-Pr case Nu increases with any small tilt of a RBC ($\beta = 0$) or VC ($\beta = \pi/2$) cell. The global maximum of Nu is obtained for an intermediate value of β. The absolute values of Nu are smaller for smaller

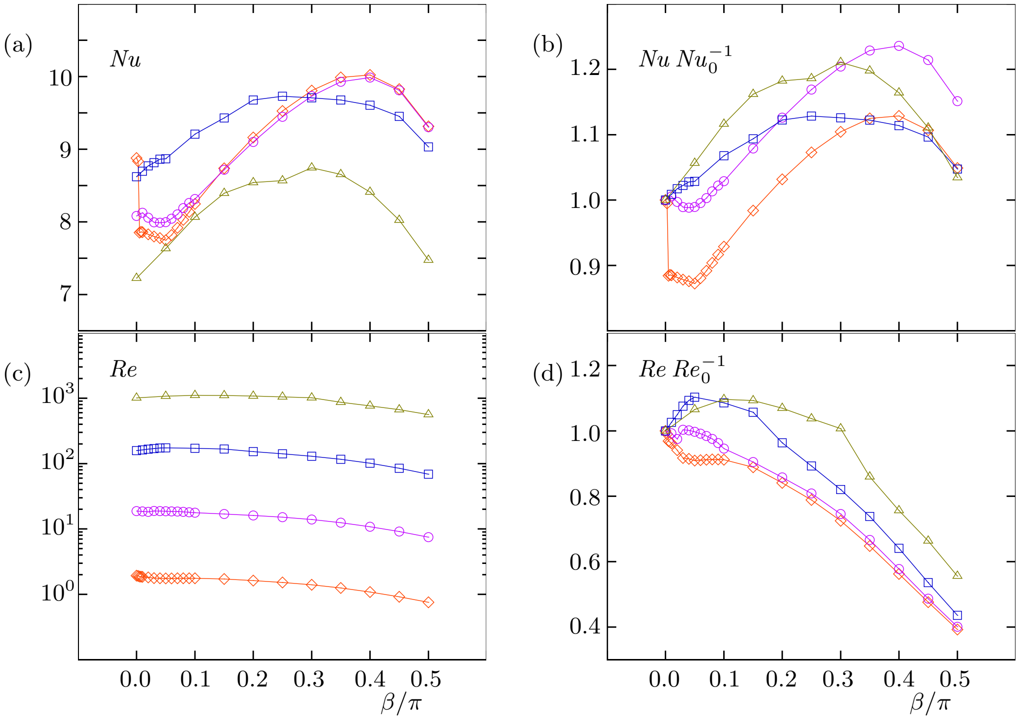

FIGURE 4. Absolute (a, c) and normalized (c, d) with the corresponding values for RBC ($\beta = 0$) Nusselt numbers (a, b) and Reynolds numbers (c, d) in inclined convection in a cylinder of the aspect ratio 1, for $Ra = 10^6$ and $Pr = 0.1$ (triangles), $Pr = 1$ (squares), $Pr = 10$ (circles) and $Pr = 100$ (diamonds), as functions of the inclination angle β.

Pr (figure 4a), but the relative increase of the mean heat transport $Nu(\beta)/Nu(0)$ is larger for smaller Pr (figure 4b).

The curves $Nu(\beta)$ for large Pr ($Pr = 10$ and $Pr = 100$) almost replicate each other for $\beta \geqslant 0.1\pi$ and differ only near $\beta = 0$. With a small tilt of the RBC cell (β close to 0) a tiny increase of Nu is possible. This effect is similar to that found by Weiss & Ahlers (2013) in their measurements in water. With further inclination of the cell, the $Nu(\beta)$-curve turns down; this drop of the Nusselt number is better pronounced for larger Pr. For $Ra = 10^6$ already by $\beta \approx 0.05\pi$ the value of $Nu(\beta)$ starts to grow till $\beta \approx 0.4\pi$, where it reaches its global maximum and after that it decreases with growing β till $\beta = \pi/2$.

The Reynolds numbers are presented in the figures 4(c) and 4(d). On a log-scale the general behaviour of Re seems similar for all Pr, however, the normalised Reynolds numbers, $Re(\beta)/Re(0)$, reveal a very different dependence on the cell tilt, especially for small β. Remarkably, for $Pr = 0.1$ and 1 the Reynolds number increases while for $Pr = 100$ it decreases, and for $Pr = 10$, $Re(\beta)/Re(0)$ drops, increases, and then drops again.

Both curves for $Pr = 10$ and for $Pr = 100$ show a couple of kinks which can be related to the different preferred large-scale flow states which can be steady or oscillatory. For $Pr = 1$ the initial increase with β is related to unsteady convection and a sufficiently efficient buoyancy-induced mixing of the bulk. For larger tilting angles $0.05\pi \lesssim \beta \lesssim 0.15\pi$ the flow stabilises, and an oscillating LSC develops that is reflected in the slow decrease in Re. Finally, for completely steady convection at $\beta \gtrsim 0.15$, $Re(\beta)/Re(0)$ decreases,

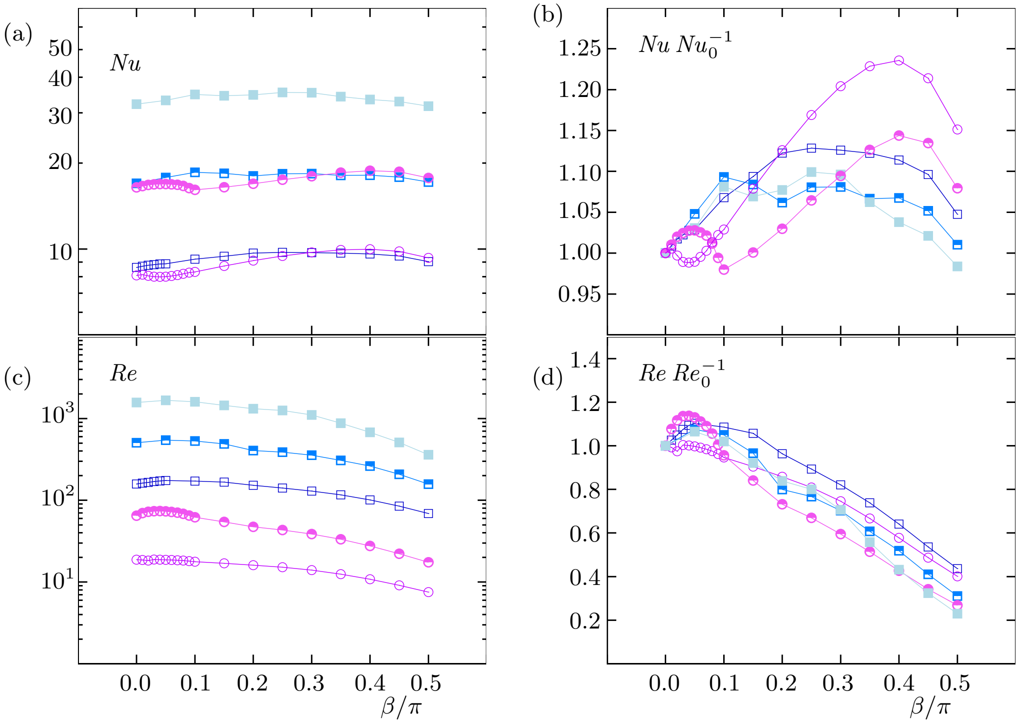

FIGURE 5. Absolute (a, c) and normalized (c, d) with the corresponding values for RBC ($\beta = 0$) Nusselt numbers (a, b) and Reynolds numbers (c, d) in inclined convection in a cylinder of the aspect ratio 1, for $Pr = 1$ (squares) and $Pr = 10$ (circles), and $Ra = 10^6$ (open symbols), $Ra = 10^7$ (half filled symbols) and $Ra = 10^8$ (filled symbols), as functions of the inclination angle β.

but now much sharper. Similarly, for $Pr = 0.1$, the initial increase up to $\beta \approx 0.15\pi$ is due to the unsteady mixing in the bulk. The competing effect of stratification caused by the inclination then leads first to a gentle down-slope. Eventually, for $\beta \gtrsim 0.3\pi$, the flow becomes steady and $Re(\beta)/Re(0)$ drops abruptly. Hence, in all cases $Re(\beta)/Re(0)$ decreases with growing β near $\beta = \pi/2$ (VC state) with similar slope. This decrease is only slightly steeper for larger Pr.

The Rayleigh number is besides Pr evidently the other important control parameter that influences the Nu- and Re-dependencies on inclined thermal convection. Thus, we conducted DNS for $Pr = 1$ where we varied Ra from 10^6 to 10^8, and DNS for $Pr = 10$ with $Ra = 10^6$ and 10^7. The results are shown in figure 5.

As expected, for almost all considered Ra, $Nu(\beta)/Nu(0)$ grows near $\beta = 0$ and decreases near $\beta = \pi/2$, see figure 5(a)–(b). Otherwise, the curves do not show a very distinct or apparent regularity dependent on Ra. The principle structure of the $Nu(\beta)/Nu(0)$-profiles (figure 5(b)) is determined mainly by Pr. For $Pr = 1$, the function $Nu(\beta)/Nu(0)$ has one maximum for $Ra = 10^6$ and at least two maxima and one minimum for $Ra = 10^7$ and $Ra = 10^8$. The first maxima for $Ra = 10^7$ and 10^8 are at about the same β. However, the heat transfer is most efficient at an inclination of $\beta = 0.25\pi$ for $Ra = 10^6$ and $Ra = 10^8$, but closer to the RBC case at $\beta = 0.1\pi$ for $Ra = 10^7$.

A $Pr = 10$ fluid behaves differently. In both studied cases, for $Ra = 10^6$ and $Ra = 10^7$, the heat transport is most efficient for $\beta = 0.4\pi$, i.e. closer to VC. For $Ra = 10^7$ there is

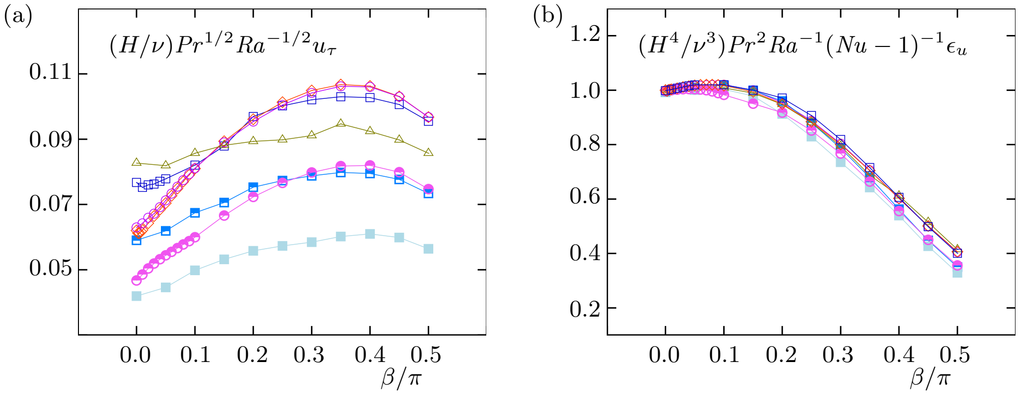

FIGURE 6. Normalized (a) friction velocity u_τ, averaged in time and over the top and bottom plates, and (b) time- and volume-averaged kinetic dissipation rate ϵ_u, in inclined convection in a cylinder of the aspect ratio 1, for $Pr = 0.1$ (triangles), $Pr = 1$ (squares), $Pr = 10$ (circles) and $Pr = 100$ (diamonds), and $Ra = 10^6$ (open symbols), $Ra = 10^7$ (half filled symbols) and $Ra = 10^8$ (filled symbols), as functions of the inclination angle β.

another pronounced maximum at $\beta = 0.05$, albeit lower in magnitude. Contrary to that, for $Ra = 10^6$, the $Nu(\beta)/Nu(0)$ curve has a minimum at the very same β. For $Ra = 10^6$ only an almost negligable heat flux intensification can be found for small tilt angles, at the tiny angle of $\beta = 0.005\pi$.

For all Prandtl numbers considered, the Nusselt number in the VC case becomes gradually smaller relative to the RBC case, with increasing Ra; and for $Ra = 10^8$ and $Pr = 1$ it is even below it. But neither VC nor RBC seem to be clearly distinguished states in terms of the heat transport.

The Reynolds number, on the other hand, shows at least for $\beta \gtrsim 0.25\pi$ a much more regular dependence on β, see figure 5(c)–(d). For all cases, the relative Reynolds number $Re(\beta)/Re(0)$ was found to decrease near $\beta = \pi/2$, and stronger for larger Ra. Again, the largest variation of $Re(\beta)/Re(0)$ is found near $\beta = 0$: first it increases with β near $\beta = 0$ and then, after its maximum which is achieved within the inclination interval $[0; 0.1\pi]$, it gradually decreases.

In an attempt to gain some further insight into the complicated $Nu(\beta)$ and $Re(\beta)$ behaviour, we studied the friction velocity u_τ at the bottom plate, evaluated as

$$u_\tau^2 = \nu\partial_z \left(\langle u_r^2 + u_\phi^2\rangle_{z=0}\right)^{1/2}$$

and presented in figure 6(a). Contrary to the naive assumption that it should be highest for VC, since in this case the core of the fluid is stably stratified and the flow along the boundaries is a developed shear flow, the friction velocity is maximal for $\beta = 0.4\pi$. Indeed, the maximum shear velocity u_τ coincides with the maximum of Nu for large Pr. Very likely it also contributes to the intensification of Nu with decreasing β compared to the VC case for all Pr. But it is not the only mechanism, and certainly not the dominant one for smaller Pr and higher Ra. Here, the buoyancy-induced mixing and the more efficient transport by plumes along the cylinder sidewall, in particular for smaller β, seems to predominantly determine the behaviour of Nu and Re with β.

Finally, we evaluate the time- and volume-averaged kinetic dissipation rate $\epsilon_u = \langle\nu\sum_i(\nabla u_i)^2\rangle$. In the particular case of $\beta = 0$ (RBC) the following exact relation holds: $\epsilon_u = (\nu^3/H^4)Pr^{-2}Ra(Nu-1)$. With growing but still small inclination angle β, the normalised kinetic dissipation rate $(H^4/\nu^3)Pr^2Ra^{-1}(Nu-1)^{-1}\epsilon_u$ might slightly increase,

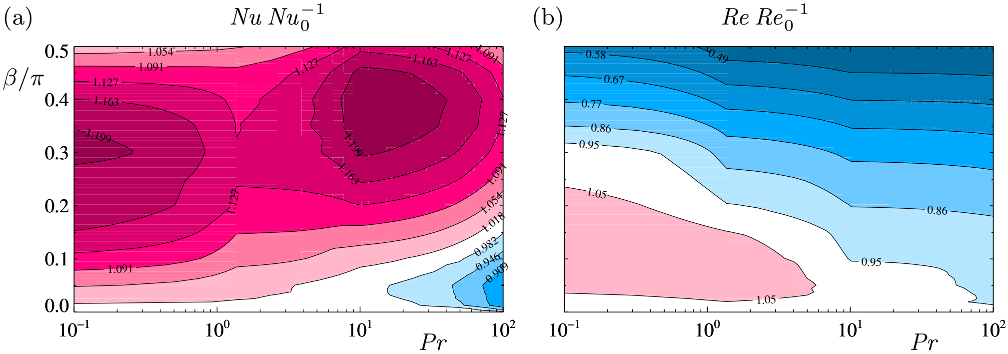

FIGURE 7. Phase diagrams for (a) $Nu\,Nu_0^{-1}$ and (b) $Re\,Re_0^{-1}$ in the $(Pr,\,\beta)$ plane, showing the regions of a relative increase (pink) or decrease (blue) of the Nusselt and Reynolds numbers with respect to the RBC case ($\beta = 0$), as it was obtained in the DNS.

but already for $\beta \geqslant 0.1\pi$ it gradually decreases with growing β in all studied cases. The β-dependencies of the normalised ϵ_u are presented in figure 6(b). In all cases these dependences look very similar and demonstrate a $\approx 60\%$ decrease of the normalised volume-averaged kinetic dissipation rate in VC, compared to that in RBC.

3. Discussion

The conducted DNS show that the Nusselt number and Reynolds number dependencies in inclined convection are generally non-monotonic complicated functions of Ra and Pr. Obviously, the geometry of the convection cell also influences these dependences. The results are summarised in figure 7, where phase diagrams for $Nu\,Nu_0^{-1}$ and $Re\,Re_0^{-1}$ are presented in the $(Pr,\,\beta)$ plane. These diagrams show the regions of relative deviations of Nu and Re with the respect to the RBC case ($\beta = 0$), as it was obtained in the DNS.

In contrast to RBC ($\beta = 0$), in VC ($\beta = \pi/2$) the turbulent processes are much weaker, but the LSC is more coherent. In both limiting cases the heat transport is generally not as effective as in inclined convection, as it was obtained in all cases studied here ($Ra \leqslant 10^8$).

For small-Prandtl-number fluids, the velocity of the LSC (reflected in Re) starts to increase with β already for a tiny tilt of the RBC cell, which leads to a more effective heat transport. Thus, a felicitous combination of buoyancy and shear in IC in fluids with $Pr \ll 1$ can lead to a significant increase of the mean heat flux, as it was obtained by Frick *et al.* (2015); Kolesnichenko *et al.* (2015). The increase of Nu compared to that in the RBC case is found to be larger for smaller Pr and higher Ra.

Contrary to the small-Pr fluid flows, for large Pr, a maximum of $Re(\beta)$ is obtained close to $\beta = 0$. The absolute increase of the LSC velocity due to the cell inclination is small, if any, and after a possible maximum the Reynolds number decreases gradually with increasing β. This drop of Re is stronger for larger Ra. Thus, in large-Pr fluids by high Ra, an increase of the heat transport due to an additional shear is not expected, and this is supported by a recent experiment by Guo *et al.* (2015), where a gradual decrease of Nu with the cell inclination was obtained for $Pr \approx 6.7$ and $Ra \approx 4.4 \times 10^9$. We anticipate further, that for larger Ra and $Pr > 1$, the decrease of $Nu(\beta)$ with increasing β will be better pronounced by the following reasons. As our simulations show, for larger β, the onset of turbulence requires larger Ra. Therefore, for the same Ra the flow can be already in the fully turbulent regime in the case $\beta = 0$ (RBC) and still in the laminar or transitional regime in the case $\beta = \pi/2$ (VC). Since the scaling exponents in the Nu-vs.-Ra scaling are generally larger for the turbulent regimes (Grossmann & Lohse 2000;

Schlichting & Gersten 2000), the ratio of the Nusselt number at $\beta = \pi/2$ to the Nusselt number at $\beta = 0$ will gradually decrease with growing Ra in that range. The behaviour of $Nu(\beta)$ in large-Pr fluids near $\beta = 0$ is quite complicated. A non-monotonicity of $Nu(\beta)$ in that region cannot be explained exclusively by a single- or multiple-roll structure of LSC, as the non-monotonic dependencies were obtained also in the regions where a clear dominance of a single-roll global flow structure was observed.

The complicated behaviour of the Nu vs. Ra dependence, with multiple extrema, in the studied range of Ra and Pr can be explained by the interaction of different transitions. Thus, for a fixed parameter $\beta = 0$ (RBC), the flow can vary from a steady one for small Ra to a turbulent one for large Ra. Even when two parameters are fixed, namely, the Rayleigh number at a certain moderate value and $\beta = 0$, the flow can be turbulent for small Pr (Frick *et al.* 2015; Horn & Shishkina 2015; Shishkina *et al.* 2013, 2014) or non-turbulent (irregularly or periodically time dependent) for large Pr (Krishnamurti 1970; Bosbach *et al.* 2012; Horn & Shishkina 2014; Horn *et al.* 2013). When also the parameter β varies, the situation becomes even more complicated, as with growing β the onset of turbulence moves to larger Ra. Moreover, with changing β, the flow symmetries change, which influence the $Nu(Ra, Pr, \beta)$ and $Re(Ra, Pr, \beta)$ dependences (see also Wei *et al.* (2015) on sharp transitions in RBC, caused by changes of flow symmetries).

For larger Ra, where the convection flows are turbulent for all β, the dependences should be simpler. As discussed, for large Ra we expect a monotonic reduction of Nu with growing β for large Pr, as in the experiments by Guo *et al.* (2015), and a single maximum for an intermediate value of β in the Nu vs. β dependence for the case of small Pr, as it was obtained in the measurements by Frick *et al.* (2015); Kolesnichenko *et al.* (2015); Langebach & Haberstroh (2014); Vasil'ev *et al.* (2015). Further investigations of inclined convection in different fluids, both, experimentally and numerically, for large and small Pr, are required for a better understanding of the IC driving mechanisms and its $Re(\beta)$- and $Nu(\beta)$-dependences.

OS is grateful to Guenter Ahlers, Eberhard Bodenschatz, Peter Frick, Detlef Lohse and Stephan Weiss for fruitful discussions. The authors acknowledge Leibniz Supercomputing Centre (LRZ) for providing computing time. OS acknowledges also financial support of the Deutsche Forschungsgemeinschaft (DFG) under the grant Sh405/4 – Heisenberg fellowship.

REFERENCES

Ahlers, G., Brown, E. & Nikolaenko, A. 2006 The search for slow transients, and the effect of imperfect vertical alignment, in turbulent Rayleigh–Bénard convection. *J. Fluid Mech.* **557**, 347–367.

Ahlers, G., Grossmann, S. & Lohse, D. 2009 Heat transfer and large scale dynamics in turbulent Rayleigh–Bénard convection. *Rev. Mod. Phys.* **81**, 503–537.

Bodenschatz, E., Pesch, W. & Ahlers, G. 2000 Recent developments in Rayleigh–Bénard convection. *Annu. Rev. Fluid Mech.* **32**, 709–778.

Bosbach, J., Weiss, S. & Ahlers, G. 2012 Plume fragmentation by bulk interactions in turbulent rayleigh–bénard convection. *Phys. Rev. Lett.* **108**, 054501.

Brown, E. & Ahlers, G. 2006 Rotations and cessations of the large-scale circulation in turbulent Rayleigh–Bénard convection. *J. Fluid Mech.* **568**, 351–386.

Castaing, B., Gunaratne, G., Heslot, F., Kadanoff, L., Libchaber, A., Thomae, S., Wu, X.-Z., Zaleski, S. & Zanetti, G. 1989 Scaling of hard thermal turbulence in Rayleigh–Bénard convection. *J. Fluid Mech.* **204**, 1–30.

Chillà, F., Rastello, M., Chaumat, S. & Castaing, B. 2004 Long relaxation times and tilt sensitivity in Rayleigh–Bénard turbulence. *Eur. Phys. J. B* **40** (2), 223–227.

Chillà, F. & Schumacher, J. 2012 New perspectives in turbulent Rayleigh–Bénard convection. *Eur. Phys. J. E* **35**, 58.

Ciliberto, S., Cioni, S. & Laroche, C. 1996 Large-scale flow properties of turbulent thermal convection. *Phys. Rev. E* **54**, R5901–R5904.

Cioni, S., Ciliberto, S. & Sommeria, J. 1997 Strongly turbulent Rayleigh–Bénard convection in mercury: Comparison with results at moderate Prandtl number. *J. Fluid Mech.* **335**, 111–140.

Frick, P., Khalilov, R., Kolesnichenko, I., Mamykin, A., Pakholkov, V., Pavlinov, A. & Rogozhkin, S. A. 2015 Turbulent convective heat transfer in a long cylinder with liquid sodium. *Europhys. Lett.* **109**, 14002.

Grossmann, S. & Lohse, D. 2000 Scaling in thermal convection: A unifying view. *J. Fluid Mech.* **407**, 27–56.

Guo, S.-X., Zhou, S.-Q., Cen, X.-R., Qu, L., Lu, Y.-Z., Sun, L. & Shang, X.-D. 2015 The effect of cell tilting on turbulent thermal convection in a rectangular cell. *J. Fluid Mech.* **762**, 273–287.

Horn, S. & Shishkina, O. 2014 Rotating non-Oberbeck–Boussinesq Rayleigh-Bénard convection in water. *Phys. Fluids* **26**, 055111.

Horn, S. & Shishkina, O. 2015 Toroidal and poloidal energy in rotating Rayleigh–Bénard convection. *J. Fluid Mech.* **762**, 232–255.

Horn, S., Shishkina, O. & Wagner, C. 2013 On non-Oberbeck–Boussinesq effects in three-dimensional Rayleigh–Bénard convection in glycerol. *J. Fluid Mech.* **724**, 175–202.

Kolesnichenko, I.V., Mamykin, A. D., Pavlinov, A. M., Pakholkov, V. V., Rogozhkin, S. A., Frick, P. G., Khalilov, R. I. & Shepelev, S. F. 2015 Experimental study on free convection of sodium in a long cylinder. *Thermal Engineering* **62**, 414–422.

Krishnamurti, R. 1970 On the transition to turbulent convection. Part 2. The transition to time-dependent flow. *J. Fluid Mech.* **42**, 309–320.

Langebach, R. & Haberstroh, C. 2014 Natural convection in inclined pipes - a new correlation for heat transfer estimations. *AIP Conference Proceedings*, vol. 1573, pp. 1504–1511.

Lohse, D. & Xia, K.-Q. 2010 Small-scale properties of turbulent Rayleigh–Bénard convection. *Annu. Rev. Fluid Mech.* **42**, 335–364.

Ng, C. S., Ooi, A., Lohse, D. & Chung, D. 2015 Vertical natural convection: application of the unifying theory of thermal convection. *J. Fluid Mech.* **764**, 0349–361.

Roche, P.-E., Gauthier, F., Kaiser, R. & Salort, J. 2010 On the triggering of the ultimate regime of convection. *New J. Phys.* **12** (8), 085014.

Schlichting, H. & Gersten, K. 2000 *Boundary-Layer Theory*, 8th edn. Springer.

Shishkina, O., Horn, S. & Wagner, S. 2013 Falkner-Skan boundary layer approximation in Rayleigh–Bénard convection. *J. Fluid Mech.* **730**, 442–463.

Shishkina, O., Horn, S., Wagner, S. & Ching, E. S. C. 2015 Thermal boundary layer equation for turbulent Rayleigh–Bénard convection. *Phys. Rev. Lett.* **114**, 114302.

Shishkina, O., Stevens, R. J. A. M., Grossmann, S. & Lohse, D. 2010 Boundary layer structure in turbulent thermal convection and its consequences for the required numerical resolution. *New J. Phys.* **12**, 075022.

Shishkina, O. & Wagner, S. 2016 Prandtl-number dependence of heat transport in laminar horizontal convection. *Phys. Rev. Lett.* **116**.

Shishkina, O., Wagner, S. & Horn, S. 2014 Influence of the angle between the wind and the isothermal surfaces on the boundary layer structures in turbulent thermal convection. *Phys. Rev. E* **89**, 033014.

Siggia, E. 1994 High Rayleigh number convection. *Annu. Rev. Fluid Mech.* **26**, 137–168.

Sun, C., Xi, H.-D. & Xia, K.-Q. 2005 Azimuthal symmetry, flow dynamics, and heat transport in turbulent thermal convection in a cylinder with an aspect ratio of 0.5. *Phys. Rev. Lett.* **95**, 074502.

Vasil'ev, A. Yu., Kolesnichenko, I. V., Mamykin, A. D., Frick, P. G., Khalilov, R. I., Rogozhkin, S. A. & Pakholkov, V. V. 2015 Turbulent convective heat transfer in an inclined tube filled with sodium. *Technical Physics* **60**, 1063–7842.

Wei, P., Weiss, S. & Ahlers, G. 2015 Multiple transitions in rotating turbulent rayleigh–bénard convection. *Phys. Rev. Lett.* **114**, 114506.

Wei, P. & Xia, K.-Q. 2013 Viscous boundary layer properties in turbulent thermal convection in a cylindrical cell: the effect of cell tilting. *J. Fluid Mech.* **720**, 140–168.

Weiss, S. & Ahlers, G. 2013 Effect of tilting on turbulent convection: cylindrical samples with aspect ratio γ=0.50. *J. Fluid Mech.* **715**, 314–334.